Earthquakes and Structures, *Vol. 12, No. 2 (2017) 191-200*
DOI: https://doi.org/10.12989/eas.2017.12.2.191

Nonlinear static and dynamic behavior of reinforced concrete steel-braced frames

Reyhaneh Eskandari[1a], Davoud Vafaei*[1], Javid Vafaei[2b] and Mohammad Ebrahim Shemshadian[3c]

[1]*Department of Civil Engineering, Chabahar Maritime University, Chabahar, Iran*
[2]*Department of Civil and Environmental Engineering, Amirkabir University of Technology, Tehran, Iran*
[3]*Department of Civil, Environmental, and Geo-Engineering, University of Minnesota (Twin Cities), Minneapolis, USA*

(Received October 15, 2015, Revised January 6, 2017, Accepted January 18, 2017)

Abstract. In this paper, the seismic performance of reinforced concrete braced frames (RC-BF) under far- and near-fault motions was investigated. Four-, eight-, 12- and 16-story RC-BFs were designed on the basis of a code-design method for a high risk seismic zone. Nonlinear static and dynamic analyses of the frames have been performed using OpenSees software. To consider diverse characteristics of near-fault motions, records with forward-directivity and fling-step effects were employed. From the results obtained in the analytical study it is concluded that the used design method was reasonable and the mean maximum drift of the frames under all ground motion sets were in acceptable range. For intermediate- and high-rise buildings the near-fault motions imposed higher demands than far-faults.

Keywords: reinforced concrete; steel-brace; dual system; nonlinear analysis; far- and near-fault motions

1. Introduction

Dual system of reinforced concrete (RC) moment frame with concrete shear walls has been used as a common lateral load resisting system in design of different multi-story buildings in many earthquake prone countries, like USA, New Zealand and Iran. The behavior of structural systems with contribution of RC-shear walls has been the subject of a number of current research studies (Beiraghi *et al*. 2015, Bekő *et al*. 2015, Jünemann *et al*. 2016, Li *et al*. 2015, Mostofinejad and Mohammadi Anaei 2012, Saad *et al*. 2016, Wang *et al*. 2016). Although this system has many advantages, it is not without problems. Heavy weight, large footprint, somewhat difficult to construct, large lateral stiffness and relatively high weight-to-strength ratio and most importantly developing tension cracks and compression crushing and spalling under large inelastic cyclic displacements are some of these. The tension cracking and compression spalling can result in serious deterioration of stiffness and reduction in strength (Zhao and Astaneh-Asl 2004). In order to resolving these problems, steel bracing of RC frames was investigated by some researchers and nowadays bracing system is one of the most effective systems to improve the seismic performance of reinforced concrete frames.

Most of the published studies analytically evaluated the use of steel bracing systems for retrofitting seismically inadequate reinforced concrete frames, such as (Abou-Elfath and Ghobarah 2000, Badoux and Jirsa 1990, Del Valle 1980, Del Valle *et al*. 1988, El-Amoury and Ghobarah 2005, Foutch *et al*. 1989, Tena-Colunga *et al*. 1996, Viswanath *et al*. 2010). These analytical studies mentioned that steel bracing is very well suited for lateral strengthening and/or stiffening of multistory reinforced concrete structures.

In case of experimental investigations, the similar observations were reported and the efficiency of bracing system in improving performance of RC frames was shown (Bush *et al*. 1991, Ghaffarzadeh and Maheri 2006, Huang *et al*. 2014, Ju *et al*. 2014, Maheri and Ghaffarzadeh 2008, Maheri and Sahebi 1997, Youssef *et al*. 2007).

Surveying literature reveals that there is little reported works which consider structures composed of reinforced concrete frames and steel bracings as a dual system. Malekpour *et al*. (2013) utilized a direct displacement-based design procedure to design dual system of RC-BFs. The results demonstrated the efficiency of this procedure by satisfying Life Safety performance level of all designed frames (Malekpour *et al*. 2013). Massumi and Absalan (2013) assessed the interaction between bracing system and moment resisting frame in braced RC frames. They used the results of experimental tests to make and calibrating micro-models of experimental specimens with complete details in ANSYS software. The results showed that the interaction between RC frame and bracing system had a positive and significant impact on improving the behavior of dual system (Massumi and Absalan 2013).

The seismic behavior factor (R) of steel X-braced and knee-braced RC buildings evaluated using inelastic

*Corresponding author, Lecturer
E-mail: d.vafaei@cmu.ac.ir
[a]Lecturer
E-mail: r.eskandari@cmu.ac.ir
[b]MSc.
E-mail: jvafaie@gmail.com
[c]Ph.D. Student
E-mail: shems003@umn.edu

Copyright © 2017 Techno-Press, Ltd.

ISSN: 2092-7614 (Print), 2092-7622 (Online)

pushover analysis by Maheri and Akbari (2003). Similar study on steel chevron-braced RC frames was done by Akbari and Maheri in 2011. Since in designing dual systems, the share of bracing system from the base shear is an important parameter, they designed steel bracing systems for three different shares of base shear (0, 50 and 100%). The RC frame designed to resist the remaining base shear. The results showed that it was beneficial to apportion the base shear between the X-bracing system and RC frame more evenly. Also for different ductility demands of dual system tentative R values proposed (Akbari and Maheri 2011, Maheri and Akbari 2003).

Godínez-Domínguez and Tena-Colunga (2010) conducted nonlinear static analyses to evaluate the behavior of 4 to 24 stories ductile moment-resisting reinforced concrete concentric braced frame structures (RC-MRCBFs) using chevron steel bracing. RC-MRCBFs designed using a capacity design methodology adapted to the general requirements of the seismic, reinforced concrete and steel guidelines of Mexico's Federal District Code (MFDC-04). In order to had a comprehensive study for each building they utilized three different values for the lateral strength balance between the bracing system and the moment frame. Up to 25%, up to 50% and nearly 75% of the lateral shear strength provided by the columns of the RC moment-resisting frame and the bracing system provided the rest. Based on this research, the capacity design methodology used by the authors was successful to design ductile RC-MRCBFs when the columns of the moment frames resist at least 50% of the total seismic shear force, without the contribution of the bracing system. Also, in this research some key design parameters, such as story drift at yielding, ultimate drift capacities, and overstrength reduction factors, were proposed (Godínez-Domínguez and Tena-Colunga 2010). Pursuing their previous study, Godínez-Domínguez *et al*. (2012) published their findings for case studies on the seismic behavior of RC-MRCBFs. The study mentioned that if capacity design principles and specific design parameters for the new design of reinforced concrete chevron braced framed were utilized, appropriate global ductility capacities and overstrength demands were achieved, and a reasonable structural performance was obtained (Godínez-Domínguez *et al*. 2012).

Although a huge body of knowledge obtained from abovementioned studies, but there is a lack of information about the global performance of this system, especially in the proximity of an active fault. So, this study focuses on the seismic performance of the dual RC diagonal steel braced system. To address this issue, four-story, eight-story, 12-story and 16-story RC-BFs were designed for a high seismically active area in accordance with Iranian Seismic Design Code (4rth Edition (2014)), Iranian reinforced concrete structures design code and Iranian steel structures design code. OpenSees software was employed for nonlinear static and dynamic analyses. Utilized earthquake records were carefully selected so as to reflect characteristics of ordinary far-fault records and typical near-fault records having forward-directivity and fling-step effects.

2. Design of model structures

To evaluate seismic performance of reinforced concrete braced frames, four frames with different heights were designed in compliance with three specifications namely, Iranian Seismic Design Code (4rth Edition (2014)), Iranian reinforced concrete structures design code and Iranian steel structures design code. Structural models are four-story, eight-story, 12-story, and 16-story RC-BFs with four 6 m spans in each direction and 3.2 m story height. Exterior RC frames with contribution of steel braces were used to resist lateral seismic loads and interior frames were assumed to carry only gravity loads. The plan view and the elevation of the designed perimeter RC braced frames are shown in Fig. 1. Dead and live (or snow) loads of 6 kN/m^2 and 1.5 kN/m^2 were used in roof level and 6 kN/m^2 and 2 kN/m^2 were used in second levels for gravity loads. In all models steel type ST37 with nominal yield strength equal to 235.4 MPa was used for braces. The compressive strength of $\acute{f}_c = 24.53$ MPa for the concrete and yielding stress equal to 412 MPa for the steel reinforcement was assumed. The below mentioned design procedure was considered for seismically design of the frames.

1) Determination of the design factors.

2) Determination of the design equivalent lateral force.

3) Determination of the percentage of the lateral shear strength provided separately by the steel bracing system and moment frame.

4) Design braces for their percentage from the lateral shear force.

5) Determination of the column sizes and resulting axial load ratios (important for column ductility)

6) Design beams and columns for their percentage from the lateral shear force by considering strong column-weak beam principle even if code does not require it.

7) Control the maximum allowable interstory drift for dual system.

It is noticeable that some of these steps iterated for several times to earn the best design by guaranteeing the expected collapse mechanism of strong column–weak beam-weaker brace.

The frames designed for regions with seismic high hazard level and stiff soil site condition (class D based on FEMA356 soil classification). According to Iranian seismic design code the design base shear is determined as follows

$$V = C.W \quad \Rightarrow \quad C = \frac{A \times B_1 \times N \times I}{R_u} \tag{1}$$

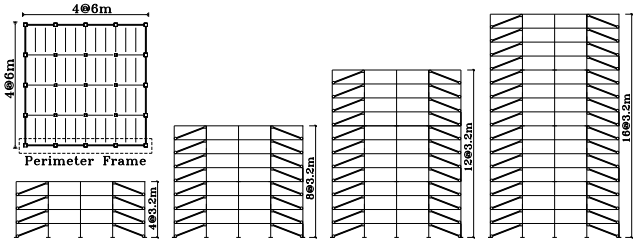

Fig. 1 Plan and elevation of the designed perimeter RC braced buildings

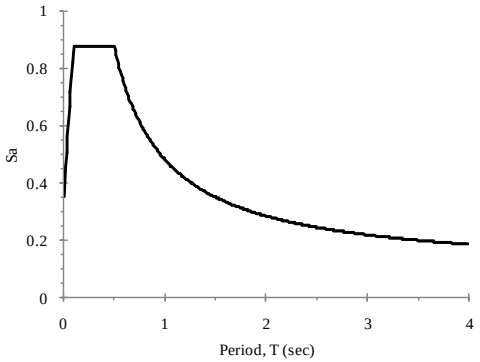

Fig. 2 Design spectra for seismic high hazard zone according to Iranian Seismic Design Code

where V is base shear force of structure, C is seismic coefficient and W is the equivalent weight of the structure which is equal to total dead load plus percentage of live load. $A \times B_1 \times N$ is the design spectral acceleration (S_a), which depends on the seismic hazard level of the site, soil type and fundamental period of the structure (T). N is the correction factor to incorporate the near-fault earthquake effects on the response spectrum shape. I is the importance factor and R_u is the response modification factor.

The assumptions of seismic design parameters included stiff soil, importance factor of one (for residential building), response modification factors of 6 and seismic zone factor (A) of 0.35. The corresponding acceleration design spectrum is depicted in Fig. 2.

In order to have a ductile structure, the RC frame is designed to sustain up to 50 percent of the lateral loads and bracing system designed to resist the remaining, on the bases of findings of Maheri and Akbari (2003) and Godínez-Domínguez and Tena-Colunga (2010).

For the first elements, steel braces were designed. Seismically compacted box sections were employed and the limiting slenderness ratios for special concentric braced frames, proposed by Iranian steel structures design code (which is similar to other international codes (AISC360-05 2005, UBC-97 1997)), were considered in the design of these elements.

Since the flexural behavior of columns depends on the level of axial compression force of columns, to gain reasonable ductility it was necessary to limit the axial force of these elements. So, the initial cross sections of the columns were calculated based on the maximum expected axial forces transmitted from braces to columns (P_u) by taking into account the following limitation

$$A_g > \frac{P_u}{0.5 f_c'} \tag{2}$$

To finalize the columns design and determining geometric characteristics of the beams with their reinforcements, elastic analysis were conducted on bare RC frames. These frames were designed on the basis of strong column-weak beam principle by checking $\sum M_c > 1.2 \sum M_b$ at each joint. In this formula which established in Iranian reinforced concrete structures design code, $\sum M_c$ is the sum of moment design value of the top and bottom column end on the joint. $\sum M_b$ is the sum of moment design value of the left and right beam end on the joint. In case of shear design of the elements, adequate reinforcement determined to prevent a nonductile shear failure before developing full flexural strength of member. It is worth noting that lateral reinforcement of RC elements tends to improve ductility by preventing premature shear failures and by confining the compression zone. More detailed description of design procedure can be found in Godínez-Domínguez and Tena-Colunga (2010).

3. Development of building models

After designing previously stated frames, nonlinear static and dynamic analyses should be performed to investigate system behavior under diverse characteristics of earthquakes. So, it is necessary to construct nonlinear accurate models to carry out the analyses. This modeling was carried out with the aim of nonlinear modeling capabilities of the Open Source for Earthquake Engineering Simulation (OpenSees) software developed by the PEER Center (Mazzoni *et al*. 2007). The computer simulation of braces and RC elements with their assumptions made are presented in the following.

3.1 Steel brace modeling

In order to model bracing elements in a way that make it possible to capture post buckling behavior of these elements, nonlinear beam-column element using fiber sections was employed. Since in the formulation of this element both usual and geometric stiffness matrix was contributed, it is capable of predicting linear or nonlinear buckling of braces during severe earthquakes (Asgarian *et*

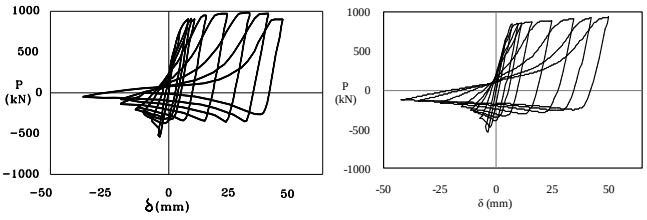

Fig. 3 Hysteretic response of HSS 4×4×1/4 hollow strut, (a) Experimental (Black *et al*. 1980), (b) analytical

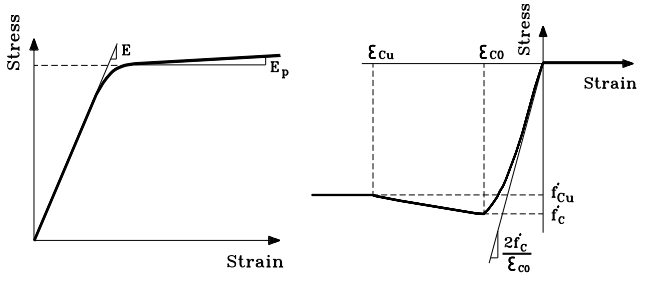

Fig. 4 Employed models for, (a) Steel, (b) Concrete

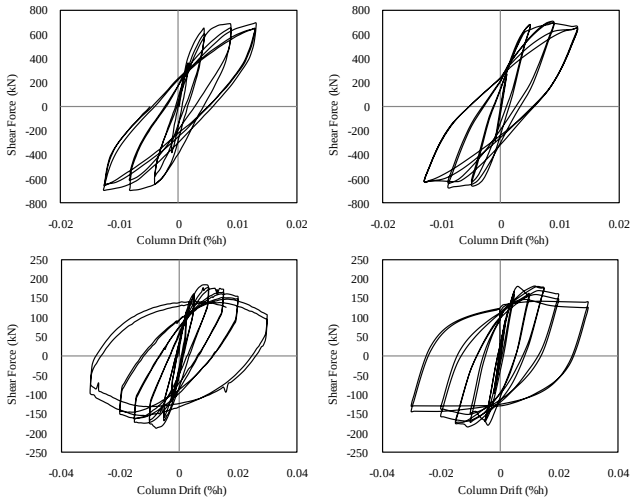

(a) (b)

Fig. 5 Comparison of experimental and analytical results, (a) Experimental (Gill *et al*. 1979, Kono and Watanabe 2002), (b) analytical

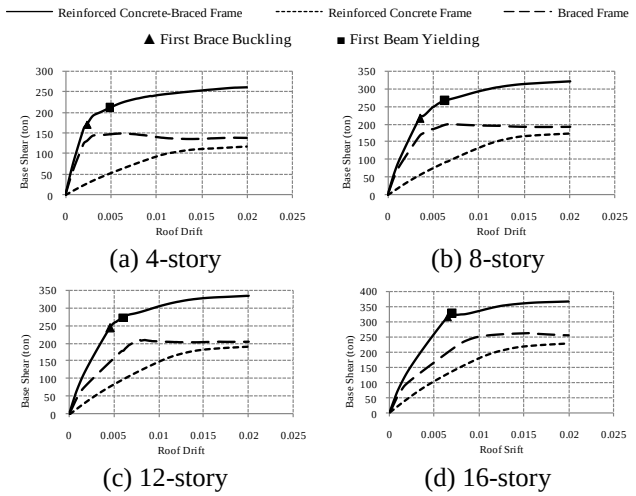

(a) 4-story (b) 8-story

(c) 12-story (d) 16-story

Fig. 6 Pushover analysis results for 4-, 8-, 12- and 16-story RC-BFs

al. 2005, Uriz *et al*. 2008). Large displacement effects were considered in model through the corotational transformation approach proposed by Crisfield (Crisfield 1991). The Giuffre-Menegotto-Pinto material (Steel02) was assigned to braces. An initial imperfection equal to 0.005 of the length of the elements was implemented in the middle of each brace length to trigger overall buckling in these elements (Farahi and Mofid 2013 ; Uriz and Mahin 2008). The trigger overall buckling in these elements (Farahi and Mofid 2013 ; Uriz and Mahin 2008). The comparison of experimental with analytical results for a hollow HSS 4×4×1/4 strut, modeled in abovementioned way, under a cyclic loading has been shown in Fig. 3.

3.2 RC elements modeling

To model all RC beams and columns the nonlinear beam-column element that utilizes a layered fiber section was used. Ten points of integration were used along each element length in each step of the analysis. This model captures the cracking behavior of the concrete section using a uniaxial concrete constitutive law, and tracks the spread of plasticity through the element cross section and along the element length. It also captures the axial-flexural interaction, automatically. A significant limitation of the fiber model is its inability to simulate the collapse behavior of a ductile RC frame. Consequently this problem is one of the limitations of the model, which may be considered in the future studies. The fibers in each cross section were assigned material properties to represent either unconfined concrete, confined concrete, or steel reinforcement. The confined strength and stress-strain behavior of the concrete was determined on the basis of Mander model (Mander *et al*. 1988).

For reinforcing steel, from the library of materials introduced in OpenSees, 'Steel02' material was assigned. On the other hand, a no tensile strength uniaxial material which is based on Kent-Scott-Park (1971) model was taken into consideration to simulate the inelastic behavior of both confined and unconfined concrete. Stress-strain curve of utilized models are depicted in Fig. 4.

Fardis and Biskinis (2003) estimate that approximately 35% of the plastic-rotation capacity of RC elements comes from the strain penetration or bond-slip of the longitudinal reinforcing bars (Fardis and Biskinis 2003). In order to provide an analytical model by considering these effects, a bond-slip spring in series with the fiber element was used to capture the bond-slip deformations up to flexural yielding and the steel strain-hardening stiffness was adjusted to capture bond-slip and shear flexibility in the post-yield regime. Additional information about modeling details can be found in Peer Report 2007/12 (Haselton *et al*. 2007). In order to validate the prediction accuracy of the mentioned analytical model, the experimental studies by Gill et al. (test No. 4) (Gill *et al*. 1979) and Kono and Watanabe (test No. D1N60) (Kono and Watanabe 2002) were employed. The excellent agreement between the numerical results and the corresponding experimental measurements in Fig. 5 is observed.

For the dynamic evaluations, one half of the total building mass was applied to the frame and distributed proportionally to the floor nodes. Furthermore, the Newmark method with integration parameters of γ=0.5 and β=0.25 was utilized to solve the equations of motion. In the dynamic analysis, the 5% Rayleigh damping was specified in the first and third modes.

4. Numerical analysis

Static-pushover analyses were performed to ensure similar system strength between the bare RC and braced frames designs and to investigate the relative stiffness of each frame type. It is noticeable that braced frames have non-moment beam-to-column connection. The pushover analyses used the lateral force distribution prescribed by the equivalent lateral force procedure (Iranian Seismic Design Code). The static-pushover curves of the frames with a

Table 1 Characteristics of selected ground motions

No.	Year	Earthquake	Mw	R^2 (km)	Mech.[1]	Station	PGA (g)	PGV (cm/s)
a) *Far-Fault motions*								
FF1	1952	Kern county	7.5	36.2	TH/REV	Taft	0.18	17.50
FF2	1994	Northridge	6.7	23.7	TH	Century CCC	0.26	21.19
FF3	1992	Big Bear	6.4	40.1	SS	Desert Hot Spr. (New Fire Stn.)	0.23	19.14
FF4	1994	Northridge	6.7	26.4	TH	Moorpark (Ventura Fire Stn.)	0.29	20.97
FF5	1994	Northridge	6.7	26.9	TH	Saturn Street School	0.43	43.52
FF6	1971	San Fernando	6.6	23.5	TH	Castaic, Old Ridge Route	0.27	25.90
FF7	1992	Landers	7.3	85.0	SS	Baker	0.11	9.42
FF8	1989	Loma Prieta	7.0	67.4	OB	Presidio	0.10	12.91
FF9	1994	Northridge	6.7	57.5	TH	Terminal Island Fire Stn. 111	0.19	12.09
FF10	1994	Northridge	6.7	44.2	TH	Montebello	0.18	9.41
b) *Near-Fault motions (Forward-Rupture Directivity)*								
NF-FWD1	1979	Imperial-Valley	6.5	5.6	SS	El Centro Diff. Array	0.35	71.23
NF-FWD2	1984	Morgan Hill	6.1	1.5	SS	Coyote Lake Dam	1.16	80.29
NF-FWD3	1989	Loma Prieta	7.0	5.1	OB	Corralitos	0.64	55.20
NF-FWD4	1989	Loma Prieta	7.0	4.5	OB	Gilroy STA #2	0.37	32.92
NF-FWD5	1992	Erzincan	6.7	2.0	SS	Erzincan	0.50	64.32
NF-FWD6	1992	Cape Mendocino	7.1	15.9	TH	Petrolia, General Store	0.66	90.16
NF-FWD7	1994	Northridge	6.7	8.6	TH	Rinaldi Rec. Stn.	0.84	174.79
NF-FWD8	1994	Northridge	6.7	6.2	TH	Jensen Filt. Plant	0.42	106.30
NF-FWD9	1999	Kocaeli	7.4	11.0	SS	Duzce	0.31	58.85
NF-FWD10	1987	Superstition Hills	6.4	0.7	SS	Parachute Test Site	0.45	112.00
c) *Near-Fault motions (Fling-Step)*								
NF-FS1	1999	Kocaeli	7.4	3.2	SS	Sakarya	0.41	82.05
NF-FS2	1999	Chi-Chi	7.6	3.0	TH	TCU068	0.50	277.56
NF-FS3	1999	Chi-Chi	7.6	7.9	TH	TCU072	0.46	83.60
NF-FS4	1999	Chi-Chi	7.6	13.8	TH	TCU074	0.59	68.90
NF-FS5	1999	Chi-Chi	7.6	11.4	TH	TCU084	0.98	140.43
NF-FS6	1999	Chi-Chi	7.6	2.2	TH	TCU129	0.98	66.92
NF-FS7	1999	Chi-Chi	7.6	4.5	TH	TCU082	0.22	50.49
NF-FS8	1999	Chi-Chi	7.6	8.3	TH	TCU078	0.43	41.88
NF-FS9	1999	Chi-Chi	7.6	3.2	TH	TCU076	0.33	65.93
NF-FS10	1999	Chi-Chi	7.6	11.0	TH	TCU079	0.57	68.06

[1]*Faulting Mechanism=TH: Thrust; REV: Reverse; SS: Strike-slip; OB: Oblique*

[2]*Closest distance to fault*

sequence of yield attainments by the frame members are provided in Fig. 6. From the results obtained by the analyses it is indicated that braced frames are stiffer than bare RC frames when designed to have equal strength. At first, buckling occurs in braces (shown by symbol ▲). Then, the beams reach their moment yield limit (shown by symbol ■). The models are continually pushed over to reach the 2% roof drift. With increasing number of stories the first brace buckling step and first beam hinging step are going to be closer and occur in nearly the same roof displacement. The first yield point of the beam in 4-, 8-, 12- and 16-story frames occurs when the roof displacement of the frame is 2.06, 1.76, 1.33 and 1.07 times of those of first brace buckling, respectively. These results are in good agreement with the results obtained by Godínez-Domínguez and Tena-Colunga (2010). It is also confirmed with pushover results that the bare RC and braced models had almost similar elastic strength (lateral load at first buckling /yielding), as was intended.

Dynamic analyses using 30 scaled earthquake ground motions were performed for each model. The selected earthquakes consist of 10 ordinary far-fault records, 10 near-fault ground motions having forward-directivity and 10 near-fault ground motions having fling effects. Forward-directivity and fling-step are two main characteristics of near-fault ground motions. The effects of these characteristics on different kinds of buildings were assessed in several studies (Eskandari and Vafaei 2015, Kalkan and Kunnath 2006, Vafaei and Eskandari 2015, 2016). In this study, to have a comprehensive study with considering diverse characteristics of earthquakes, these records were utilized. Many of the employed records were used by Kalkan and Kunnath (2007) (Kalkan and Kunnath 2007). Pertinent information on the ground motion data sets are summarized in Table 1. Ground motions were scaled to match the design spectra with minimum error in the period range of 0.6 s to 4.0 s. In Fig. 7 the scaled acceleration spectra for each ten earthquake records, along with the design acceleration spectrum for the site is presented.

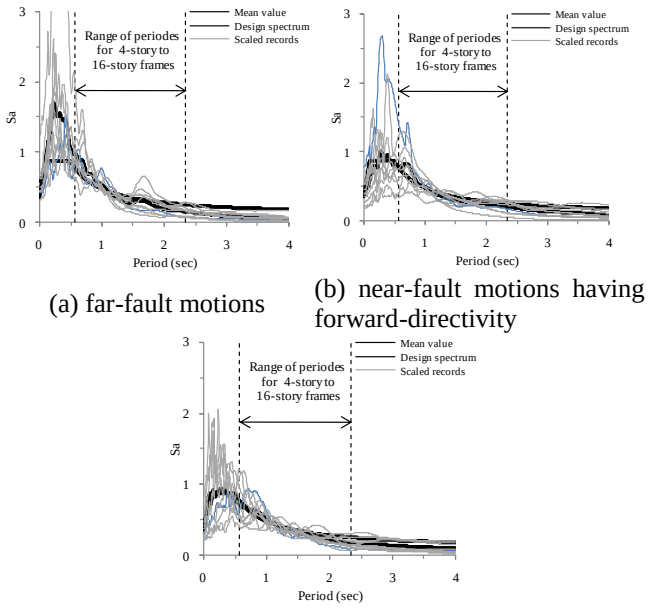

(a) far-fault motions

(b) near-fault motions having forward-directivity

(c) near-fault motions having fling-step

Fig. 7 Design spectrum and individual earthquake spectra (5% damping)

Since the maximum interstory drift ratio (IDR) can present an appropriate measure for the evaluation of damages inflicted by the Earthquake on the structural and non-structural components, in the present study this quantity is used as the primary measure of seismic demand. The maximum IDR of the four-, eight-, 12- and 16-story RC-BFs are presented in Figs. 8 and 9. For the four-story frames under most of the records, regardless of their characteristics, nearly similar profiles were produced. Because the first mode of vibration was dominant, the largest demand is generally concentrated at the lower story levels. The largest demand is caused by the NF-FWD3 record, which produced a 2.03 percent interstory drift at the second story.

For the eight story buildings, the similar profiles were shown for all the far-fault records, whereas the results of near-fault records were so disperse. The maximum IDR of the first story level of these frames subjected to forward-directivity earthquakes was varying from (NF-FWD2) 0.21% to (NF-FWD8) 2.81%. For records with fling effects, the similar results were observed. The peak IDR of three sets of records at the critical floor that is caused by FF10, NF-FWD8, and NF-FS9 records were 1.41%, 2.81% and 2.36%, respectively. For all records, the maximum demand distributed uniformly throughout the frame heights, and all floor components were utilized to dissipate seismic input energy.

In case of 12- and 16-story high-rise frames similar observations were shown. Although due to predominant effects of higher modes the maximum IDR was occurred in upper floors, but the IDR of the other stories were significant too. The results dispersion for near-fault motions was significant and they imposed higher demands than far-faults, especially records having forward-directivity effects.

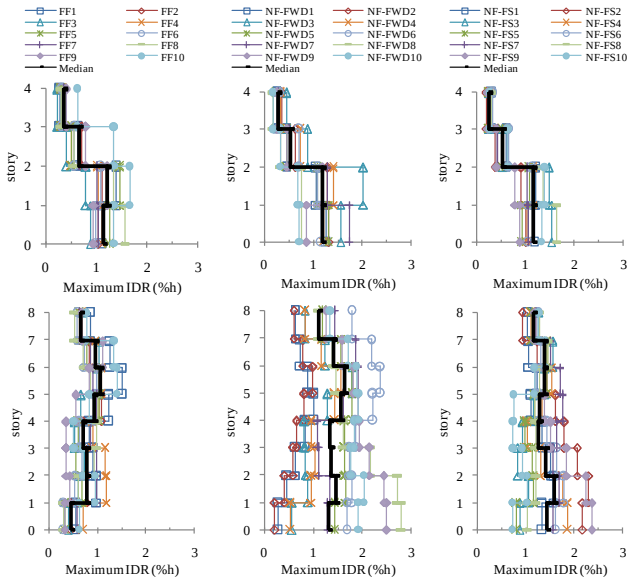

(a) (b) (c)

Fig. 8 Max interstory drift of four-story and eight-story RC-braced frames for (a) far-fault motions, (b) near-fault motions having forward directivity effects (c) near-fault motions having fling effects

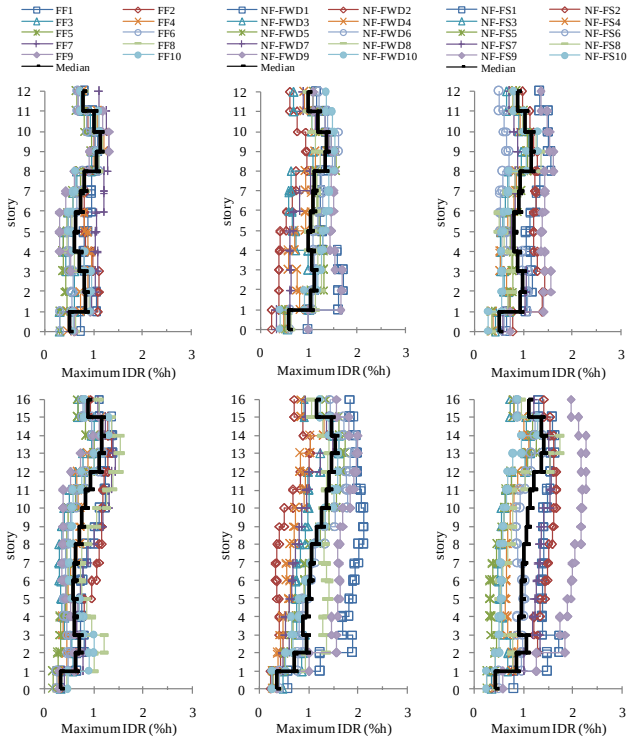

(a) (b) (c)

Fig. 9 Max interstory drift of 12-story and 16-story RC-braced frames for (a) far-fault motions, (b) near-fault motions having forward directivity effects (c) near-fault motions having fling effects

Of the entire data set, the NF-FWD1 record generated the highest demand, 1.73 and 1.84 percent interstory drift for 12- and 16-story frames, respectively. Finally, from the observations of the IDR profiles it is indicated that all RC-braced frames under each set of motions had reasonable mean maximum drift values (less than 2%).

As mentioned earlier, in the design of the dual system it is assumed that each of the RC and braced frames could resist one half of the story shear, separately. To assessment each systems contribution from the story shear in the dual system, the ratio of mean of lateral shear forces resisted by columns to total story shear for each RC-braced frame is presented in Fig. 10. To gain comprehensive insight, the results were presented in the various IDR ranges. For low values of the IDR, i.e. IDR<0.5%, due to higher initial stiffness of the braced frames, the columns lateral resisted forces was so less than half (about 26% of the total story shear). By increasing the IDR values the columns contribution from the shear force were increased. For 0.5<IDR<1, 1<IDR<1.5 and IDR more than 1.5 percent the columns share from lateral loads were 31%, 42% and 47%, respectively, and the rest was provided by the bracing system. These results demonstrated that for IDR more than 1% the shear force distributed almost evenly between columns and braces.

In order to assessment the sequence of yield/buckle attainments by the frame members, the first yielding/buckling times of the elements are presented in Fig. 11. The results are for 12-story building in which

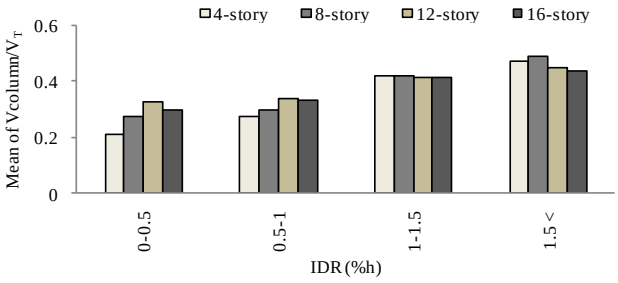

Fig. 10 The ratio of lateral shear forces resisted by columns to total story shear for 4-, 8-, 12- and 16-story RC-braced frames

the largest demand among each earthquake category was caused by FF7, NF-FWD1 and NF-FS9 records. Although the presented results were for 12-story frames, these observations were generalizable to the entire frames and all records.

For frame under far-fault record (FF7), the first element which bucked/yielded was the brace of the second story level. It was buckled at 13.98th second of the record (t_s=13.98 s). Then the buckling/yielding propagated to other elements of the frame. The results of each floor indicate that the brace buckles earlier than beam hinging. The last yielding was occurred in columns of 3rd and 4th story level at t_f=27.02 s. In case of near-fault motions (NF-FWD1 and NF-FS9) similar results were observed and at each story the first buckling/yielding was belong to the braces. In velocity time histories of Fig. 11 the times of the first and last buckling/yielding of the components were specified with t_s and t_f. For near-fault records of NF-FWD1 and NF-FS9 the difference of t_s and t_f was less than far-fault records, and plastification of the elements were occurred by a single high amplitude velocity pulses (releasing abrupt energy in a short period of time); Whereas, in velocity time history of FF7 record many reversed cycles were shown. Following previous figure, the elements yielding mappings of the same building and same records are presented in Fig. 12. In this figure, θ/θ_{cu} is the ratio of the plastic rotation demand to the plastic rotation capacity of the component, which θ_{cu} was calculated with empirical equations provided by (Panagiotakos and Fardis 2001); and L_p is the magnitude of the buckling length, which defines the failure of the brace.

From observations of this figure, it is revealed that collapse mechanisms for models subjected to a far-or near-fault motion (regardless of the type of the record) correlate reasonably well with the expected failure mechanism of strong column–weak beam–weaker brace. At each story level the first plastic deformation was occurred in a brace element. Besides the inelastic bucking of the braces significant plastic rotations for beams and some columns were shown. The results caused by near-fault motions were much more and they imposed higher demands than far-faults. The maximum plastic rotation of the beams for FF7, NF-FWD1 and NF-FS9 records are $0.55\theta_{cu}$, $0.81\theta_{cu}$ and $0.79\theta_{cu}$, respectively. These rotations produced at the elements of the 10th, third and 9th floor of the 12-story frame, which respectively 1.31, 1.73 and 1.66 percent of drifts was shown. According to these findings it is obvious

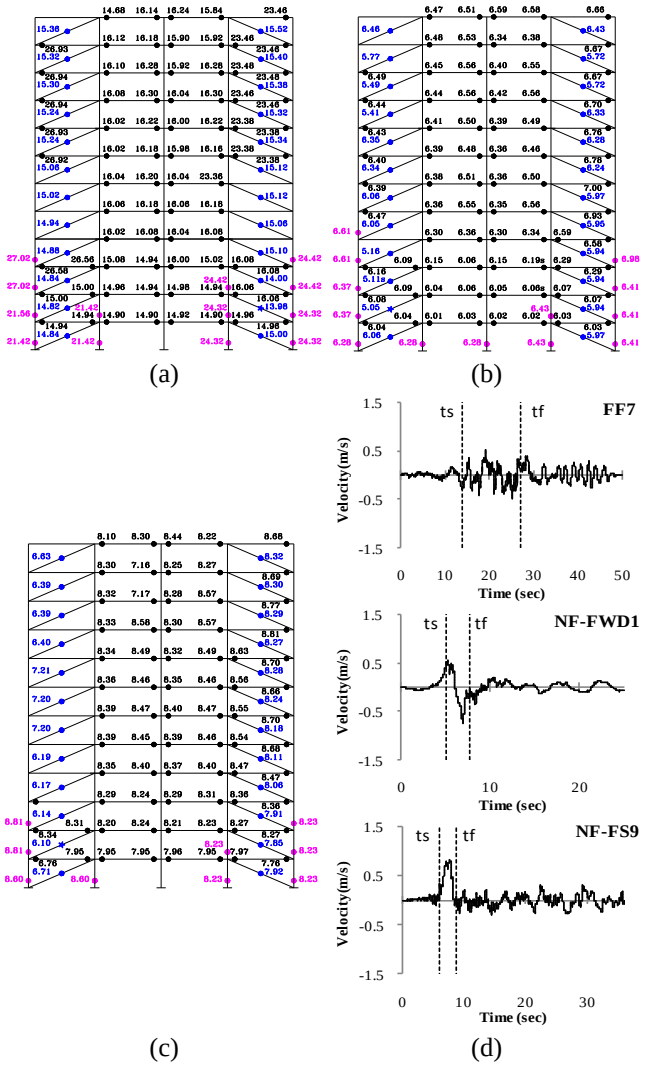

Fig. 11 Plastification in the 12-story frame under (a) typical far-fault ground motion (FF7), (b) typical near-fault ground motion with forward-directivity effect (NF-FWD1), (c) typical near-fault ground motion with fling-step effect (NF-FS9) (d) velocity time histories

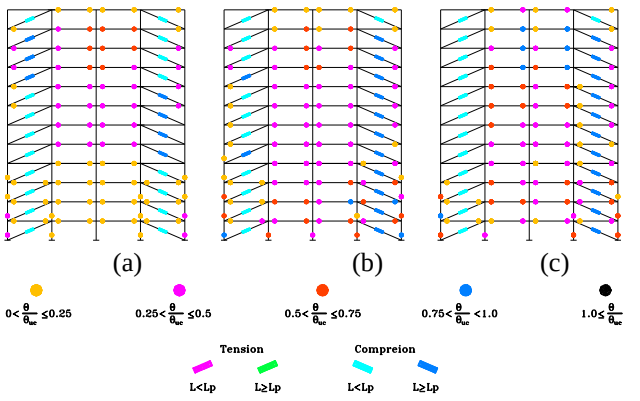

Fig. 12 Mapping of accumulated plastic rotations for 12 story frame under (a) typical far-fault ground motion (FF7), (b) typical near-fault ground motion with forward-directivity effect (NF-FWD1), (c) typical near-fault ground motion with fling-step effect (NF-FS9)

that very large drifts are not obtained by free. Review the IDR profiles in Figs. 8 and 9 reveals that under several destructive near-fault records the frames (especially 8-story one) may collapse before obtaining high IDR values.

In case of columns, plastic hinge rotations observed in just some of the lower stories. These plastic rotations have smaller magnitude respect to those obtained in beams. Plastic hinge rotations in columns at their base were unavoidable, because of the fixed-base modeling assumption, but they are usually small.

5. Conclusions

In this study, a code-design method was utilized to design the dual system of reinforced concrete braced frames. The nonlinear performance of the designed frames was evaluated by utilizing static-pushover analyses and dynamic analyses. The earthquake recordings were carefully compiled so as to reflect characteristics of normal far-fault records and typical near-fault records having forward-directivity and fling effects. The following can be concluded from the research:

The utilized code-design method was reasonable and the mean maximum IDR of the frames under all ground motion sets were in acceptable range (less than 2%).

Collapse mechanisms for models, regardless of the type of the record, correlate reasonably well with the expected failure mechanism of strong column-weak beam-weaker brace.

Near-fault records in some cases were more destructive. Generally, these motions imposed higher demands than far-faults on all frames, with exception of 4-story frame which the results of far- and near-fault records were nearer. For low-rise frames due to more effects of first mode the largest demands were occurred in lower stories. For intermediate- and high-rise frames, though due to predominant effects of higher modes the maximum IDR was occurred in upper floors, the IDR of the other stories were significant too. The maximum demand distributed uniformly throughout the frame heights, and all floor components were utilized to dissipate seismic input energy.

For intermediate- and high-rise frames, the results dispersion for near-fault motions, especially with forward-directivity effects, was significant.

The static-pushover results indicate that braced frames (with simple beam-to-column connections) were stiffer than RC frames when designed to have equal strength.

In the dual system, for stories with IDR more than 1% the shear force distributed almost evenly between RC (columns) and braced frames.

For near-fault records the plastification of the elements were occurred by a single high amplitude velocity pulses (releasing abrupt energy in a short period of time), Whereas, in velocity time history of far-fault record many reversed cycles were shown.

Besides the inelastic bucking of the braces, significant plastic rotations for beams and some columns of the RC-braced frames were observed.

This research should be continued to gain fully understanding of the behavior of RC-BFs with considering different bracing configuration and other characteristics of the ground motions.

Acknowledgments

Financial support by the Sistan and Baluchestan Construction Engineering Organization (S&B-CEO) is gratefully acknowledged.

References

Abou-Elfath, H. and Ghobarah, A. (2000), "Behaviour of reinforced concrete frames rehabilitated with concentric steel bracing", *Can. J. Civ. Eng.*, **27**(3), 433-444.

AISC (2005), *Specification for Structural Steel Buildings*.

Akbari, R. and Maheri, M.R. (2011), "Analytical investigation of response modification (behaviour) factor, R, for reinforced concrete frames rehabilitated by steel chevron bracing", *Struct. Infrastruct. Eng.*, **9**(6), 507-515.

Asgarian, B., Aghakouchack, A.A. and Bea, R.G. (2005), "Inelastic postbuckling and cyclic behavior of tubular braces", *J. Offshore Mech. Arctic Eng.*, **127**(3), 256-262.

Badoux, M. and Jirsa, J.O. (1990), "Steel bracing of RC frames for seismic retrofitting", *J. Struct. Eng.*, **116**(1), 55-74.

Beiraghi, H., Kheyroddin, A. and Kafi, M.A. (2015), "Nonlinear fiber element analysis of a reinforced concrete shear wall subjected to earthquake records", *Iran. J. Sci. Technol. Trans. Civ. Eng.*, **39**(C2+), 409-422.

Bekő, A., Rosko, P., Wenzel, H., Pegon, P., Markovic, D. and Molina, F.J. (2015), "RC shear walls: Full-scale cyclic test, insights and derived analytical model", *Eng. Struct.*, **102**, 120-131.

Black, G.R., Wenger, B.A. and Popov, E.P. (1980), "Inelastic buckling of steel struts under cyclic load reversals", UCB/EERC-80/40, Earthquake Engineering Research Center, Berkeley, California.

Bush, T., Jones, E. and Jirsa, J. (1991), "Behavior of RC frame strengthened using structural steel bracing", *J. Struct. Eng.*, **117**(4), 1115-1126.

Crisfield, M.A. (1991), *Non-linear Finite Element Analysis of Solids and Structures*, John Wiley & Sons, Inc., New York.

Del Valle, E. (1980), "Some lessons from the March 14, 1979 earthquake in Mexico City", *7th world conference on earthquake engineering*, Istanbul, Turkey.

Del Valle, E., Foutch, D.A., Hjelmstad, K.D., Figueroa-Gutiérrez, E. and Tena-Colunga, A. (1988), "Seismic retrofit of a RC building: a case study", *9th World Conference on Earthquake Engineering*, Tokyo-Kyoto, Japan.

El-Amoury, T. and Ghobarah, A. (2005), "Retrofit of RC frames using FRP jacketing or steel bracing", *J. Seismol. Earthq. Eng.*, **7**(2), 83-94.

Eskandari, R. and Vafaei, D. (2015), "Effects of near-fault records characteristics on seismic performance of eccentrically braced frames", *Struct. Eng. Mech.*, **56**(5), 855-870.

Farahi, M. and Mofid, M. (2013), "On the quantification of seismic performance factors of Chevron Knee Bracings, in steel structures", *Eng. Struct.*, **46**, 155-164.

Fardis, M.N. and Biskinis, D.E. (2003), "Deformation capacity of RC members, as controlled by flexure or shear", Otani Symposium, 511-530.

Foutch, D.A., Hjelmstad, K.D., Calderón, E.D.V., Gutiérrez, E.F. and Downs, R.E. (1989), "The Mexico Earthquake of September 19, 1985-Case studies of seismic strengthening for

two buildings in Mexico City", *Earthq. Spectra*, **5**(1), 153-174.
Ghaffarzadeh, H. and Maheri, M.R. (2006), "Cyclic tests on the internally braced RC frames", *J. Seismol. Earthq. Eng.*, **8**(3), 177-186.
Gill, W.D., Park, R. and Priestley, M.J.N. (1979), "Ductility of rectangular reinforced concrete columns with axial load", Department of Civil Engineering, University of Canterbury, Christchurch, New Zealand.
Godínez-Domínguez, E.A. and Tena-Colunga, A. (2010), "Nonlinear behavior of code-designed reinforced concrete concentric braced frames under lateral loading", *Eng. Struct.*, **32**(4), 944-963.
Godínez-Domínguez, E.A., Tena-Colunga, A. and Pérez-Rocha, L.E. (2012), "Case studies on the seismic behavior of reinforced concrete chevron braced framed buildings", *Eng. Struct.*, **45**, 78-103.
Haselton, C.B., Goulet, C.A., Mitrani-Reiser, J., Beck, J.L., Deierlein, G.G., Porter, K.A., Stewart, J.P. and Taciroglu, E. (2007), "An assessment to benchmark the seismic performance of a code-conforming reinforced concrete moment-frame building", Pacific Earthquake Engineering Research Center.
Huang, L., Tan, H. and Yan, L. (2014), "Seismic behavior of chevron braced reinforced concrete spatial frame", *Mater. Struct.*, **48**(12), 4005-4018.
Ju, M., Lee, K.S., Sim, J. and Kwon, H. (2014), "Non-compression X-bracing system using CF anchors for seismic strengthening of RC structures. Magazine of Concrete Research", **66**(4), 159-174.
Jünemann, R., de la Llera, J.C., Hube, M.A., Vásquez, J.A. and Chacón, M.F. (2016), "Study of the damage of reinforced concrete shear walls during the 2010 Chile earthquake", *Earthq. Eng. Struct. D.*, **45**(10), 1621-1641.
Kalkan, E. and Kunnath, S.K. (2006), "Effects of fling step and forward directivity on seismic response of buildings", *Earthq. Spectra*, **22**(2), 367-390.
Kalkan, E. and Kunnath, S.K. (2007), "Assessment of current nonlinear static procedures for seismic evaluation of buildings", *Eng. Struct.*, **29**(3), 305-316.
Kono, S. and Watanabe, F. (2002), "Damage evaluation of reinforced concrete columns under multiaxial cyclic loadings", The Second U.S.-Japan Workshop on Performance-Based Earthquake Engineering Methodology for Reinfoced Concrete Building Structures.
Li, G., Zhang, F., Zhang, Y. and Li, H.-N. (2015), "Nonlinear hysteretic behavior simulation of reinforced concrete shear walls using the force analogy method", *Struct. Des. Tall Spec. Build.*, **24**(7), 504-520.
Maheri, M.R. and Akbari, R. (2003), "Seismic behaviour factor, R, for steel X-braced and knee-braced RC buildings", *Eng. Struct.*, **25**(12), 1505-1513.
Maheri, M.R. and Ghaffarzadeh, H. (2008), "Connection overstrength in steel-braced RC frames", *Eng. Struct.*, **30**(7), 1938-1948.
Maheri, M.R. and Sahebi, A. (1997), "Use of steel bracing in reinforced concrete frames", *Eng. Struct.*, **19**(12), 1018-1024.
Malekpour, S., Ghaffarzadeh, H. and Dashti, F. (2013), "Direct displacement-based design of steel-braced reinforced concrete frames", *Struct. Des. Tall Spec. Build.*, **22**(18), 1422-1438.
Mander, J., Priestley, M. and Park, R. (1988), "Theoretical stress-strain model for confined concrete", *J. Struct. Eng.*, **114**(8), 1804-1826.
Massumi, A. and Absalan, M. (2013), "Interaction between bracing system and moment resisting frame in braced RC frames", *Archiv. Civ. Mech. Eng.*, **13**(2), 260-268.
Mazzoni, S., McKenna, F., Scott, M. and Fenves, G. (2007), "OpenSees command language manual", Pacific Earthquake Engineering Research (PEER) Center.
Mostofinejad, D. and Mohammadi Anaei, M. (2012), "Effect of confining of boundary elements of slender RC shear wall by FRP composites and stirrups", *Eng. Struct.*, **41**, 1-13.
Panagiotakos, T.B. and Fardis, M.N. (2001), "Deformation of reinforced concrete members at yielding and ultimate", *Struct. J.*, **98**(2), 135-148.
Saad, G., Najjar, S. and Saddik, F. (2016), "Seismic performance of reinforced concrete shear wall buildings with underground stories", *Earthq. Struct.*, **10**(4), 965-988.
Tena-Colunga, A., Valle, E.D. and Pérez-Moreno, D. (1996), "Issues on the seismic retrofit of a building near resonant response and structural pounding", *Earthq. Spectra*, **12**(3), 567-597.
Code, U.B. (1997), "Uniform building code", In International conference of building officials, USA.
Uriz, P., Filippou, F. and Mahin, S. (2008), "Model for cyclic inelastic buckling of steel braces", *J. Struct. Eng.*, **134**(4), 619-628.
Uriz, P. and Mahin, S.A. (2008), "Toward earthquake-resistant design of concentrically braced steel-frame structures", Pacific Earthquake Engineering Research Center.
Vafaei, D. and Eskandari, R. (2015), "Seismic response of mega buckling-restrained braces subjected to fling-step and forward-directivity near-fault ground motions", *Struct. Des. Tall Spec. Build.*, **24**(9), 672-686.
Vafaei, D. and Eskandari, R. (2016), "Seismic performance of steel mega braced frames equipped with shape-memory alloy braces under near-fault earthquakes", *Struct. Des. Tall Spec. Build.*, **25**(1), 3-21.
Viswanath, K.G., Prakash, K.B. and Desai, A. (2010), "Seismic analysis of steel braced reinforced concrete frames", *Int. J. Civ. Struct. Eng.*, **1**(1), 114-122.
Wang, H., Li, G. and Huang, X. (2016), "Behavior of coupled shear walls with buckling-restrained steel plates in high-rise buildings under lateral actions", *Struct. Des. Tall Spec. Build.*, **25**(1), 22-44.
Youssef, M.A., Ghaffarzadeh, H. and Nehdi, M. (2007), "Seismic performance of RC frames with concentric internal steel bracing", *Eng. Struct.*, **29**(7), 1561-1568.
Zhao, Q. and Astaneh-Asl, A. (2004), "Cyclic behavior of an innovative steel plate shear wall system", *13th World Conference on Earthquake Engineering*, Vancouver, B.C., Canada.

List of notation

$f_c^{'}$ concrete compressive strength
$f_{cu}^{'}$ concrete crushing strength
V base shear force of structure
C seismic coefficient
W the equivalent weight of the structure which is equal to total dead load plus percentage of live load
S_a design spectral acceleration obtains from $A \times B_1 \times N$
A design base acceleration (in relation to gravity acceleration g)
B_1 response coefficient of the building
N correction factor to incorporate the near-fault earthquake effects on the response spectrum shape
T fundamental period of the structure
I importance factor
R response modification factor
A_g gross area of the column

P_u maximum expected axial force which may develop in column
M_c moment design value of the column
M_b moment design value of the beam
δ brace axial displacement
ε_{c0} concrete strain at maximum strength
ε_{cu} concrete strain at crushing strength
E initial elastic tangent
E_p post-yield tangent
t_s time of the first buckling/yielding of the first element during an earthquake
t_f time of the first buckling/yielding of the last element during an earthquake